Theoretical study of sum-frequency vibrational spectroscopy on limonene surface

ARTICLE *in* THE JOURNAL OF CHEMICAL PHYSICS · MARCH 2014

Impact Factor: 2.95 · DOI: 10.1063/1.4867575 · Source: PubMed

6 AUTHORS, INCLUDING:

Renhui Zheng
Chinese Academy of Sciences
55 PUBLICATIONS **445** CITATIONS
SEE PROFILE

Qiang Shi
Chinese Academy of Sciences
101 PUBLICATIONS **2,410** CITATIONS
SEE PROFILE

Theoretical study of sum-frequency vibrational spectroscopy on limonene surface

Ren-Hui Zheng, Wen-Mei Wei, Hao Liu, Yuan-Yuan Jing, Bo-Yang Wang, and Qiang Shi

Citation: The Journal of Chemical Physics **140**, 104702 (2014); doi: 10.1063/1.4867575
View online: http://dx.doi.org/10.1063/1.4867575
View Table of Contents: http://scitation.aip.org/content/aip/journal/jcp/140/10?ver=pdfcov
Published by the AIP Publishing

Theoretical study of sum-frequency vibrational spectroscopy on limonene surface

Ren-Hui Zheng,[1,a)] Wen-Mei Wei,[2] Hao Liu,[1] Yuan-Yuan Jing,[1] Bo-Yang Wang,[1] and Qiang Shi[1]

[1]*Beijing National Laboratory for Molecular Sciences, State Key Laboratory for Structural Chemistry of Unstable and Stable Species, Institute of Chemistry, Chinese Academy of Sciences, Zhongguancun, Beijing 100190, People's Republic of China*

[2]*Department of Chemistry, College of Basic Medicine, Anhui Medical University, Hefei, Anhui 230032, People's Republic of China*

(Received 24 December 2013; accepted 24 February 2014; published online 10 March 2014)

By combining molecule dynamics (MD) simulation and quantum chemistry computation, we calculate the surface sum-frequency vibrational spectroscopy (SFVS) of R-limonene molecules at the gas-liquid interface for SSP, PPP, and SPS polarization combinations. The distributions of the Euler angles are obtained using MD simulation, the ψ-distribution is between isotropic and Gaussian. Instead of the MD distributions, different analytical distributions such as the δ-function, Gaussian and isotropic distributions are applied to simulate surface SFVS. We find that different distributions significantly affect the absolute SFVS intensity and also influence on relative SFVS intensity, and the δ-function distribution should be used with caution when the orientation distribution is broad. Furthermore, the reason that the SPS signal is weak in reflected arrangement is discussed. © *2014 AIP Publishing LLC*. [http://dx.doi.org/10.1063/1.4867575]

I. INTRODUCTION

Surface sum-frequency vibrational spectroscopy (SFVS) has been applied to study dynamics, molecular orientation and structure at interfaces[1–7] since it was first observed by Shen *et al.*[8–11] in 1986. In SFVS, there are two input lights (IR and UV/visible lights) and one output sum-frequency light. SFVS is a combination of Raman and IR processes. SFVS can only be observed for both Raman and IR activities vibrational modes.

IR intensity is related to the electric dipole moment derivatives. There are non-resonance and resonance Raman. The IR-UV doubly resonant SFVS that corresponds to resonance Raman has been observed on surfaces[12–15] and in bulk.[15] Experiments on the IR-UV doubly resonant SFVS are few. Generally, almost all the SFVS experiments are off electronic resonance, which are related to non-resonance polarizability derivatives. They can be obtained by the sum-over-states method and time-dependent method.[16–18] When studying surface SFVS, we can assume Raman polarizabilities are symmetric and nine components are simplified to six.

SFVS is from second-order nonlinear polarizability and its 18 independent components can be calculated by quantum software. Surface SFVS can be applied to obtain the molecular orientation on surfaces. Before getting orientation, scientists should know molecular distributions. It is hard to directly know them from experiment. Thus, sometimes scientists assume the molecular distributions, which include three kinds: δ-function distribution, Gaussian distribution, and isotropic distribution. Theoretically molecule dynamics (MD) simulation can obtain the distributions without assumption. Some theoretical studies[19–31] on surface SFVS have been performed. We want to know the influence of the different distributions on SFVS and more reasonable distributions for experiment studies, which has not been investigated until now.

Recently, SFVS off electronic resonance has been done on limonene chiral liquids.[32] In Ref. 32, when the SPP and PSP combinations are applied to detect chiral SFVS spectra in bulk, the SSP, PPP, and SPS combinations are also used to study achiral spectra at interfaces. Although some studies have been done on its chiral spectra,[33] no study has been performed on surface SFVS for limonene. In Ref. 32, Belkin *et al.* pointed out when they experimentally studied SFVS in reflection arrangement for limonene surface, the achiral SPS spectrum was difficult to be detected. This indicated that the SPS surface signal is too weak to measure, which is required to be studied theoretically. In this paper, using MD simulation we achieve the Euler angle distributions and obtain the structure and orientation of R-limonene on liquid surface, then with quantum chemistry computation we calculate the molecular hyperpolarizabilities. Based on the above results, we get the effective macroscopic susceptibilities and study the influences of different distributions on the surface SFVS. The calculated results are compared with experimental ones, and we discuss the reason why the SPS signal is weak.

II. THEORY

For an azimuthally isotropic surface, the SSP, SPS, PSS, and PPP effective susceptibilities are, respectively,

$$\chi_{eff}^{(2),ssp} = L_{yy}(\omega)L_{yy}(\omega_1)L_{zz}(\omega_2)\sin\beta_2\chi_{yyz}, \qquad (1)$$

a)Author to whom correspondence should be addressed. Electronic mail: zrh@iccas.ac.cn

$$\chi_{eff}^{(2),sps} = L_{yy}(\omega)L_{zz}(\omega_1)L_{yy}(\omega_2)\sin\beta_1\chi_{yzy}, \quad (2)$$

$$\chi_{eff}^{(2),pss} = L_{zz}(\omega)L_{yy}(\omega_1)L_{yy}(\omega_2)\sin\beta\chi_{zyy}, \quad (3)$$

$$\begin{aligned}\chi_{eff}^{(2),ppp} = {} & L_{xx}(\omega)L_{xx}(\omega_1)L_{zz}(\omega_2)\cos\beta\cos\beta_1\sin\beta_2\chi_{xxz} \\ & - L_{xx}(\omega)L_{zz}(\omega_1)L_{xx}(\omega_2)\cos\beta\sin\beta_1\cos\beta_2\chi_{xzx} \\ & - L_{zz}(\omega)L_{xx}(\omega_1)L_{xx}(\omega_2)\sin\beta\cos\beta_1\cos\beta_2\chi_{zxx} \\ & + L_{zz}(\omega)L_{zz}(\omega_1)L_{zz}(\omega_2)\sin\beta\sin\beta_1\sin\beta_2\chi_{zzz},\end{aligned} \quad (4)$$

where L is Fresnel factor, β_2 and β_1 are the incident angles of the IR light and the UV/visible light, respectively, β is the transmission angle of the sum-frequency light. The experimental arrangement (see Figure 1(b)) can be found in Refs. 32 and 34, which is applied to detect both chiral and achiral signals and a little different from the traditional surface SFVS arrangement.[35] Thus, the PPP effective susceptibilities are also a little different from those in Refs. 35 and 5. The four independent nonvanishing components of the susceptibilities are χ_{zzz}, $\chi_{xzx} = \chi_{yzy}$, $\chi_{xxz} = \chi_{yyz}$, and $\chi_{zxx} = \chi_{zyy}$. χ is related to the molecular hyperpolarizabilities $\alpha^{(2)}$[5]

$$\chi_{ijk} = N_s \sum_{\xi,\eta,\zeta} \langle(\hat{i}\cdot\hat{\xi})(\hat{j}\cdot\hat{\eta})(\hat{k}\cdot\hat{\zeta})\rangle\alpha_{\xi\eta\zeta}^{(2)}, \quad (5)$$

where N_s is the surface density, $(\hat{i}, \hat{j}, \hat{k})$ are the unit vectors of the lab coordinates, $(\hat{\xi}, \hat{\eta}, \hat{\zeta})$ are the unit vectors of molecular coordinates, and the angular bracket denotes the orientational average for molecules at interfaces. When the UV/visible light is off electronic resonance and the IR light is close to the vibrational resonance, the molecular hyperpolarizabilities can be written into[32]

$$\alpha_{\xi\eta\zeta}^{(2)} = \frac{1}{2\omega_q}\frac{\partial\alpha_{\xi\eta}}{\partial Q_q}\frac{\partial\mu_\zeta}{\partial Q_q}\frac{1}{\omega_2 - \omega_q + i\Gamma_q}, \quad (6)$$

where ω_q is the molecular vibrational frequency of the qth mode, $\frac{\partial\alpha_{\xi\eta}}{\partial Q_q}$ is the Raman polarizability, $\frac{\partial\mu_\zeta}{\partial Q_q}$ is the electric dipole moment derivative, and Γ_q is the IR line width.

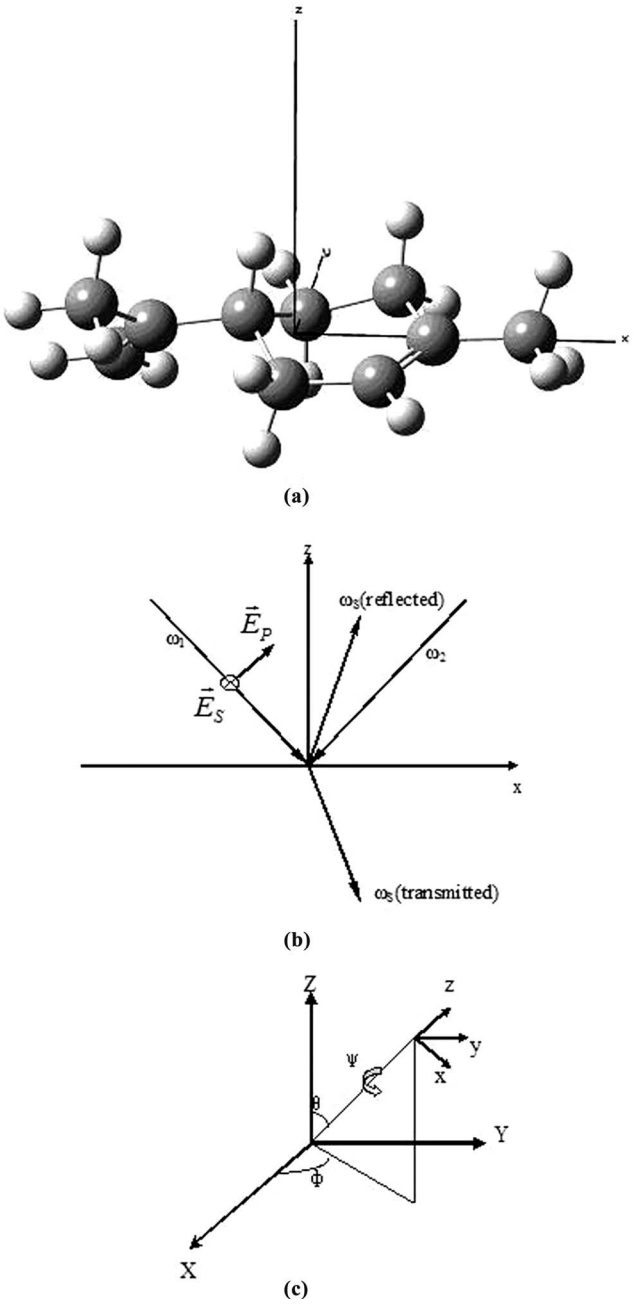

FIG. 1. (a) Molecular structure of R-limonene, (b) experimental arrangement of SFVS, and (c) Euler angles representing the rotation relation between the molecular (x,y,z) and lab coordinate (X,Y,Z) systems.

III. COMPUTATIONAL RESULTS

A. MD simulation

The force field parameters for R-limonene are generated with the following procedure: The structure is first optimized by Gaussian 09 program[36] using B3LYP/6-31G*, ESP charges for each atom are then generated at HF/6-31G* level. Finally, the ESP charges are taken to be the input of ANTECHAMBER in Amber09[37] to produce RESP charge, and other force field parameters are generated based on the generalized Amber force field (GAFF) database.[38] The simulation box which contains 500 R-limonene molecules is built by Gromacs program.[39] MD simulation is then performed at the temperature of 298 K. The simulation system is first minimized using a steepest descent algorithm. The minimized system is then equilibrated using *NPT* simulation for 6 ns. The equilibrated box size is 51.646 Å in all of the three orthogonal directions. We then add a proper vacuum volume by changing the Z direction to 102.646 Å to generate the R-limonene gas-liquid interface. *NVT* simulation of 10 ns was then performed to generate the trajectory for distribution calculations. In all the simulation, the time step is set to 2 fs, and the long-range electrostatic interactions are treated by Ewald summation.[40]

Figure 1(c) shows the definition of the Euler angles (θ,ψ,ϕ), which is used to describe the transformation between the molecular (x,y,z) and lab coordinate (X,Y,Z) systems. In Figure 2, we present the R-limonene density along the Z axis. The molecules whose density is between 90% and 10% of the bulk system are taken to be the surface. The molecule

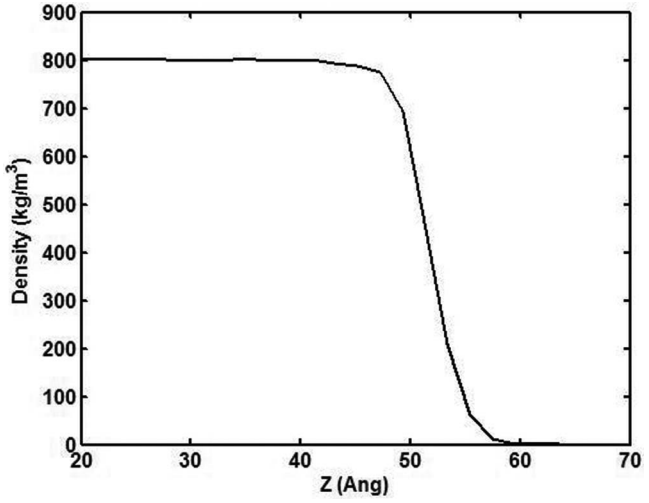

FIG. 2. Limonene density along the Z axis.

distributions are plotted in Figure 3. The θ-distribution $P(\theta)$ is antisotropic. $P(\theta)$ is in the range of 0.25–0.36, which indicates that all the orientation of R-limonene is possible at gas-liquid interfaces. The peak of $P(\theta)$ is at about 90°, which shows that the ring of R-limonene prefers to stand perpendicularly on surface. We also plot $P(\theta)\sin\theta$ in Figure 3, and we describe this distribution applying a Gaussian distribution that is $f(\theta) = 0.5435*\exp(-(\theta - 1.6729)^2/2/0.7663^2)$. ϕ-distribution is isotropic, which agrees with the result from the theoretical prediction and assumption.[41] It is strange that ψ-distribution is between Gaussian and isotropic. And we cannot describe it using only Gaussian distribution or a constant one. Generally, ψ-distribution is in the range of 0-2π. For fitting convenience, we change its distribution in the range of $-\pi$ to π. And we fit the ψ-distribution with a Gaussian function and a constant one, which is $f(\psi) = 0.0682*\exp(-(\psi + 0.0545)^2/2/1.1446^2) + 0.1282$. This distribution is peaked at about 0°. The factor 0.1282 corresponds to isotropic distribution. We name it iso-Gaussian distribution.

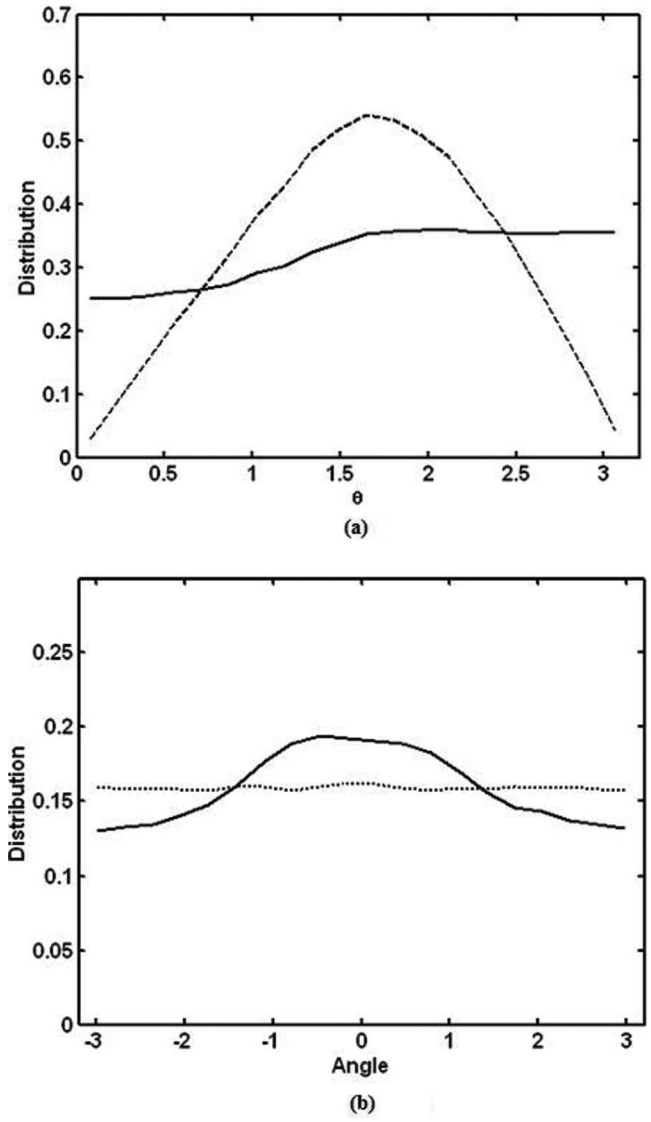

FIG. 3. (a) θ-distribution $P(\theta)$ (solid line), distribution $P(\theta)\sin(\theta)$ (dashed line), (b) ϕ-distribution (dashed-dotted line) and ψ-distribution (solid line) distribution of R-limonene molecules on the gas-liquid surface.

B. Quantum chemistry computation

In Refs. 19 and 20, Guthmuller *et al.* simulated the SFVS using different DFT, and they found that the computations done by B3LYP give the good agreement with experiment. In this work, we find the polarizabilities calculated by BLYP and B3LYP functionals give similar relative SFVS intensity, while the BLYP functional gives slightly larger absolute intensity, which agrees better with the experiment. Thus, only the BLYP results are shown in the SFVS for limonene molecule at interfaces. Using density functional theory BLYP/6-311++G** of Gaussian 09,[36] we optimize the structure of the ground state of R-limonene molecule and calculate the vibrational frequencies. Then the electric dipole moment derivatives and Raman polarizabilities with respect to the normal coordinates have been obtained. When calculating the Raman polarizabilities, we use the approximate polarizabilities. The xx, xy, yy, zx, zy, and zz components of the approximate polarizabilities for limonene molecule in standard coordinate are 213.696, 6.210, 228.311, 19.547, −4.257, and 185.185 a.u., respectively. The relation between dielectric constant ε and the polarizabilities is $\varepsilon = 1 + 4\pi N_b(\alpha_{xx} + \alpha_{yy} + \alpha_{zz})/3$, where N_b is the molecular density of bulk system. With these values and relation equation we calculate the corresponding dielectric constant, which is 2.4404. The experimental value is 2.44. The theoretical result agrees well experiment. In this work, we have not taken the anharmonicity corrections to the potential energy surface into consideration. The anharmonicity corrections impact on the vibrational frequencies and the vibrational spectra may agree better with experiment when they are taken into account. The solvent effects affect the IR and Raman intensities, which also influence the SFVS intensity. We have used the Polarizable Continuum Model (PCM) by Gaussian software to consider the solvent effects on the approximate polarizabilities of limonene molecule, the solvent effects are found to have little influence on approximate polarizabilities and the SFVS intensity.

C. Result and discussions

In the following study, the two incident angles of the IR and UV/visible lights are both taken as 45° and the angle of the sum-frequency is 30.8°.[32] We take the frequency of the visible light to be 532 nm.[32] Here, the local-field correction is chosen to be 2.2.[32,34] The molecular density is 3.7×10^{27} m^{-3}.[34] The IR linewidth Γ_q is 12 cm^{-1}.[32]

Using Eqs. (1)–(6), quantum computations and the distributions mentioned above, we compute the molecule hyperpolarizabilities and the effective SSP, PPP, and SPS susceptibilities (see Figure 4). Their intensities of the strongest peaks are about 2.0×10^{-42}, 1.7×10^{-42}, 1.6×10^{-43} m^4/V^2. Reference 34 shows that the intensity of chiral SFVS signal generated in transmission from the bulk of chiral liquid is given by

$$I(v_s) \propto \left|\chi^{bulk}_{chiral} l_c \hat{e}_s \cdot (\hat{e}_1 \times \hat{e}_2)\right|^2. \quad (7)$$

In the above equation, $\hat{e}$ is the polarization and l_c is the coherence length. In experiment,[32] the IR light and the UV/visible light overlapped at 90°. Thus in SPP spectroscopy, $\hat{e}_s \cdot (\hat{e}_1 \times \hat{e}_2)$ is almost taken to be 1. The calculated coherence length is −482 nm. From Refs. 32 and 34, we know that the chiral susceptibility for R-limonene can be 1.7×10^{-28} m^2/V^2, which is taken as unit in relative intensity in Figure 2 of Ref. 32. Also in that figure, the relative surface sum-frequency intensities of SSP, PPP, and SPS spectra are 0.08, 0.13, and 0.04, respectively. Thus, their corresponding absolute intensities are 3.1×10^{-42}, 5.4×10^{-42}, and 1.3×10^{-42} m^4/V^2, respectively. The calculated SSP signal is about 1.6 times smaller than experiment, and the calculated PPP signal is about three times smaller than experiment. The calculated SPS signal is about ten times smaller than experiment. In experiment, when Belkin *et al.*[32] measured SFVS in reflection from the surface of the limonene liquids, the achiral SPS spectrum was also hardly observable. Just as Belkin *et al.*[32] pointed out, the SPS spectrum is dominated by bulk contribution from the electric-dipole forbidden. Our calculated surface SPS signal is indeed very small and it is difficult for scientist to observe the surface SPS signal. The magnetization and quadrupole contributions may have significant influence on the SPS achiral transmitted signals.[32]

In order to investigate the SFVS under the influence of molecular distributions on the surface, we also study different distributions. First, we calculate δ-function distribution for SFVS, where the θ value is taken to be 90° and ψ is 0°. And the results are plotted in Figure 5. The magnitude of the intensities of SSP, PPP, and SPS spectra are 2.1×10^{-40}, 1.7×10^{-40}, and 5.0×10^{-41} m^4/V^2, respectively. The calculated SSP signal is about 68 times larger than experiment and the PPP signal is about 31 times larger. Moreover, the SPS signal is 38 times larger, which indicates that surface SPS signal can be observed in experiment. This is unreasonable. δ-function distribution makes the SFVS enhance for many times. In experiment, people sometimes assumed that the surface molecules are δ-distribution. The relative intensities of SFVS between the SSP and PPP signals from δ-function distribution are only a little different from those with iso-Gaussian distribution. However, those between SSP and SPS signals are larger. Different distributions affect not only the absolute SFVS intensity but also the relative SFVS intensity. From Figure 4, we see that for SSP signals the ratio of

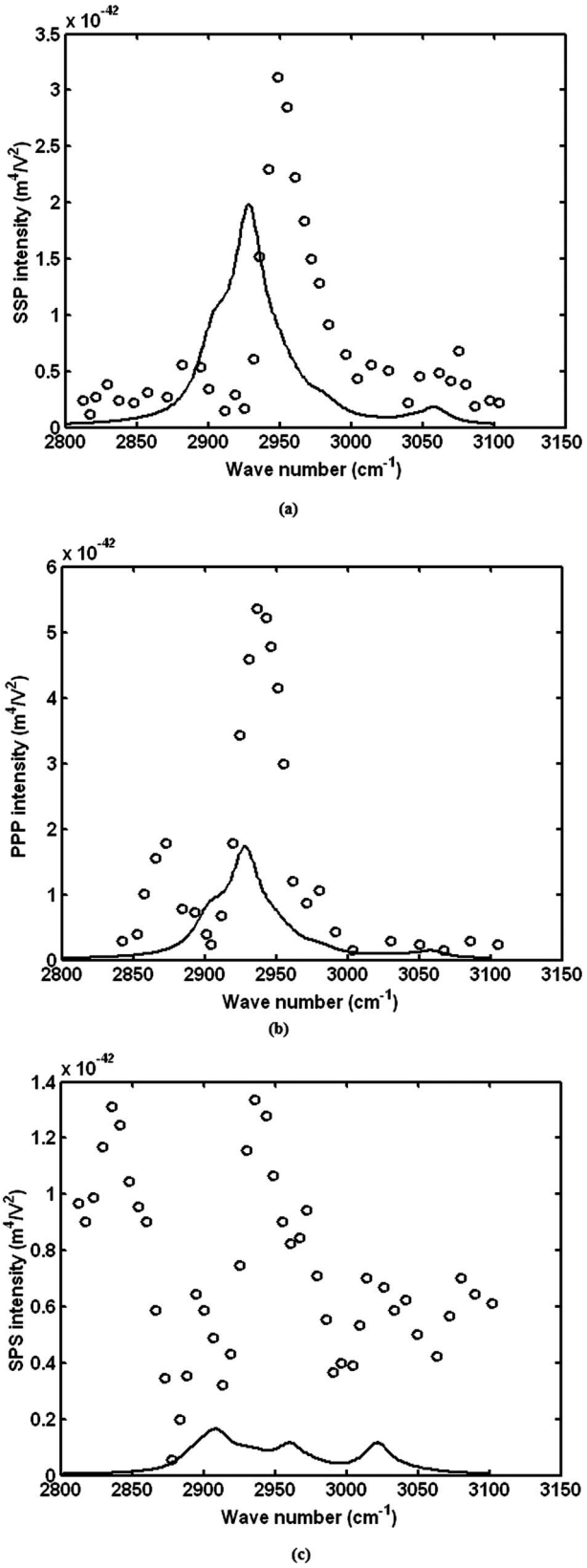

FIG. 4. (a) SSP, (b) PPP, and (c) SPS intensities of surface SFVS when the distributions of Figure 3 are applied. Open circles are data from the experiment of Ref. 32.

the SFVS intensity of the 3058 cm^{-1} mode to that of the 2928 cm^{-1} mode is 0.09. And in Figure 5, this value is 0.18. There is a new peak at 3024 cm^{-1} with an intensity of 3.4×10^{-41} m^4/V^2 (the ratio is 0.16). Thus, using δ-function distribution instead of the real distribution, experimental scientist should be careful.

In Figure 5(b), we plot SFVS using the δ-function distribution for θ with a value of 90° and isotropic distribution for ψ. The corresponding intensity is very small. The most intense peak is 6.5×10^{-45} m^4/V^2. When the isotropic distribution for ψ is applied, all the average over ψ is taken to be zero. For example, $\chi_{yyz} = \frac{1}{2}N_s(\alpha_{z'z'z'}\sin^2\theta\cos\theta + (\alpha_{x'x'z'} + \alpha_{y'y'z'})\cos\theta)$, which is zero when θ is taken to be 90°. Similarly, in the above assumption, all the effective susceptibilities are zero. Thus, the calculated SFVS is close to zero with computational errors.

In Figure 5(c), we plot SFVS using the δ-function distribution for θ with a value of 90° and iso-Gaussian distribution for ψ. The calculated SSP intensity is 2.1×10^{-42} m^4/V^2, which can be the same order of magnitude of the experimental result.[28] The calculated SSP intensity significantly depends much on the θ value. When we take it as 60°, the resulted SFVS is plotted in Figure 5(d). The SSP intensity is enhanced and can be 2.5×10^{-41} m^4/V^2, which is one order of magnitude larger than experiment.[28] We also find that their SFVS line shapes in Figure 5(d) are very different from Figures 4 and 5(a)–5(c).

Second, we apply Gaussian distribution for both θ and Ψ angles. Gaussian distribution for θ angle have been presented above and Gaussian distribution for ψ angle is shown as $f(\psi) = 0.3507*\exp(-(\psi + 0.0545)^2/2/1.1446^2)$. The calculated intensities of SSP, PPP, and SPS spectra are 3.7×10^{-41}, 3.4×10^{-41}, and 3.3×10^{-42} m^4/V^2, respectively. The calculated results are about 12 times, 6 times, and 2.5 times as large as the corresponding experimental spectra, respectively (Figure 6). The unreasonable results are that the computational surface SPS spectrum can be of the same order of magnitude of experimental one. From this, we may deduce that it is observable for the SPS polarized combination in reflected SFVS experiment, which is in contradiction with experiment.[32] Thus, only applying Gaussian distribution for ψ angle is not reasonable.

Third, we assume a Gaussian distribution for θ angle and an isotopic distribution for ψ angle. The calculated SSP, PPP, and SPS spectra are 5.3×10^{-43}, 4.3×10^{-43}, and 8.0×10^{-44} m^4/V^2, respectively (see Figure 7). The magnitude of the spectra is one or two orders smaller than that of the experimental ones.[32] More isotropic, the smaller the spectral intensity is. When the distributions of the three Euler angles are all isotropic, no surface SFVS can be observed. Detailed comparisons show that the spectral line shapes under isotropic ψ-distribution is somewhat different from the previous calculated ones.

From the above discussion, we may come to the following conclusion that the θ-distribution can be approximately Gaussian, ϕ-distribution is isotropic and ψ-distribution is between Gaussian and isotropic. In experiment, scientist assumed that ψ-distribution is δ function, Gaussian function,

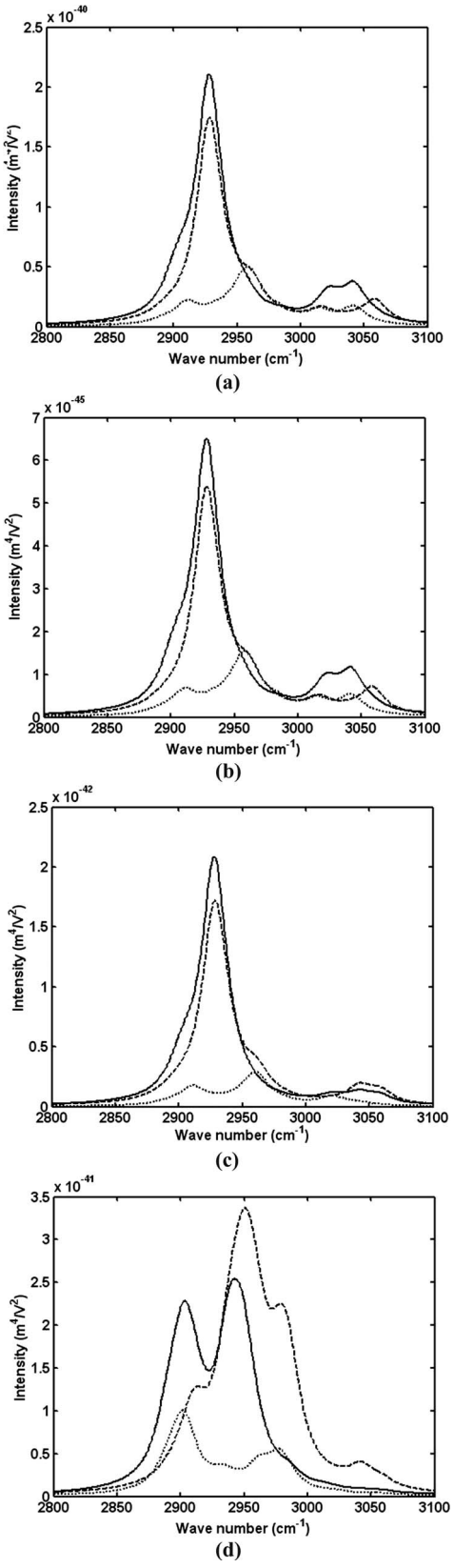

FIG. 5. SSP (solid line), PPP (dashed line), and SPS (dotted line) intensities of surface SFVS (a) when the δ-function distributions for θ (90°) and ψ (0°) angles are assumed, (b) when the δ-function distribution for θ (90°) and the isotropic distribution for ψ are assumed, (c) when the δ-function distribution for θ (90°) and the iso-Gaussian distribution for ψ are applied, (d) when the δ-function distribution for θ (60°) and the iso-Gaussian distribution for ψ are applied.

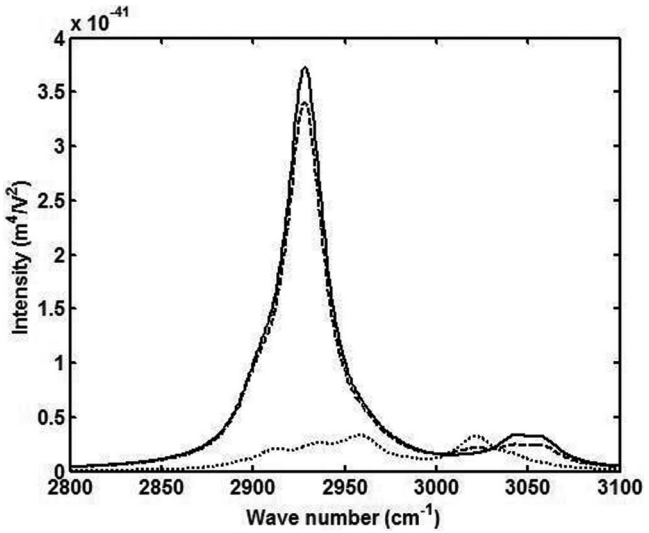

FIG. 6. SSP (solid line), PPP (dashed line), and SPS (dotted line) intensities of surface SFVS when the Gaussian distribution for ψ angle is assumed.

or constant function, which may be not the real distribution. Thus, it should be careful to assume the ψ-distribution. Previous molecular dynamics simulation also shows that acetone molecules have iso-Gaussian distribution at gas-liquid interfaces (see Figure 3 of Ref. 31).

Finally, we discuss why the surface SPS effective susceptibility is much smaller than SSP and PPP ones. There are two reasons: (i) The effective susceptibility is related to molecule polarizability, which can be expressed as the product of the Raman polarizabilities and the electric dipole moment derivatives. The SSP and PPP arrangements correspond to the diagonal Raman polarizabilities and the SPS is non-diagonal ones. Generally, diagonal Raman polarizabilities are larger than non-diagonal ones. Thus, surface SPS signal is weak. (ii) Angle distribution average also makes surface SPS signal weak. From Figures 4 and 5, we see that in a δ-function distribution the ratio between SPS and PPP spectra is 1:4, however, this ratio reduces to 1:12 in an iso-Gaussian distribution.

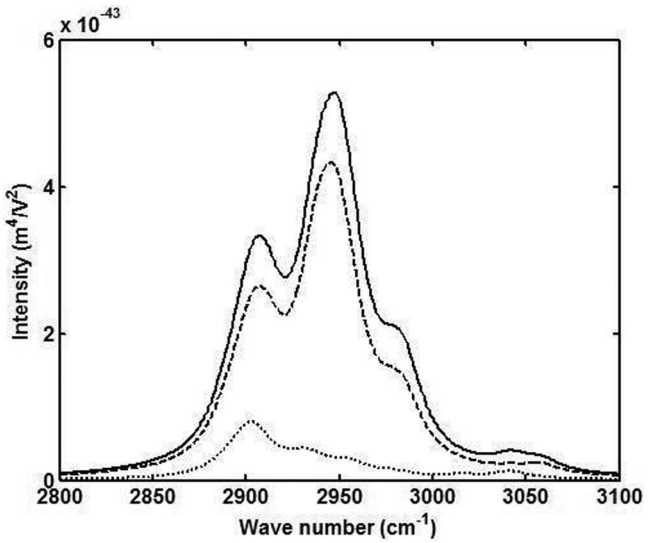

FIG. 7. SSP (solid line), PPP (dashed line), and SPS (dotted line) intensities of surface SFVS when the isotropic distribution for ψ angle is assumed.

IV. CONCLUSIONS

Using MD simulation, we study the distributions of the Euler angles for R-limonene molecules at the gas-liquid interfaces. The ϕ-distribution is isotropic, however, ψ-distribution is between Gaussian and isotropic and we name it iso-Gaussian distribution. Applying density functional theory, we calculate the corresponding Raman polarizabilities and electric dipole moment derivatives. Combining the MD simulation and quantum computation, we compute the surface SFVS for SSP, PPP, and SPS polarized combinations. Furthermore, different distributions such as δ-function distribution, Gaussian-distribution, and isotropic-distribution instead of iso-Gaussian distribution are applied to investigate surface SFVS. We find that different distributions strongly influence on the absolute SFVS intensity and also affect relative SFVS intensity, and more care should be taken into the use of the simple analytical distributions to study molecule orientation from the ratio of the SFVS intensity. Furthermore, the reason that the SPS signal is weak in reflected arrangement is analyzed. The first reason is that the susceptibility of the SPS signal is related to the non-diagonal Raman polarizabilities, which are generally smaller than diagonal ones. The second one is due to the orientation distribution of the surface molecules, which happens to reduce the SPS signal in the experimental setup in Ref. 32.

ACKNOWLEDGMENTS

This work is supported by National Natural Science Foundation of China (NNSFC) (21103003, 20903101, 91027015, 21290194), the 973 program (Grant No. 2011CB808502), and the Chinese Academy of Sciences (CAS) through the Hundred Talents project.

[1]J. A. McGuire and Y. R. Shen, Science **313**, 1945 (2006).
[2]I. V. Stiopkin, C. Weeraman, P. A. Pieniazek, F. Y. Shalhout, J. L. Skinner, and A. V. Benderskii, Nature (London) **474**, 192 (2011).
[3]J. A. Carter, Z. H. Wang, and D. D. Dlott, Acc. Chem. Res. **42**, 1343 (2009).
[4]D.-S. Zheng, Y. Wang, A.-A. Liu, and H.-F. Wang, Int. Rev. Phys. Chem. **27**, 629 (2008).
[5]H.-F. Wang, W. Gan, R. Lu, Y. Rao, and B.-H. Wu, Int. Rev. Phys. Chem. **24**, 191 (2005).
[6]G. L. Richmond, Chem. Rev. **102**, 2693 (2002).
[7]K. B. Eisenthal, Chem. Rev. **96**, 1343 (1996).
[8]X. D. Zhu, H. J. Suhr, and Y. R. Shen, J. Opt. Soc. Am. B **3**, 252 (1986).
[9]J. H. Hunt, P. Guyotsionnest, and Y. R. Shen, Chem. Phys. Lett. **133**, 189 (1987).
[10]P. Guyot-Sionnest, J. H. Hunt, and Y. R. Shen, Phys. Rev. Lett. **59**, 1597 (1987).
[11]X. D. Zhu, H. Suhr, and Y. R. Shen, Phys. Rev. B **35**, 3047 (1987).
[12]M. B. Raschke, M. Hayashi, S. H. Lin, and Y. R. Shen, Chem. Phys. Lett. **359**, 367 (2002).
[13]X. Chen, H. Tang, M. A. Even, J. Wang, G. N. Tew, and Z. Chen, J. Am. Chem. Soc. **128**, 2711 (2006).
[14]D. Wu, G.-H. Deng, Y. Guo, and H.-F. Wang, J. Phys. Chem. A **113**, 6058 (2009).
[15]M. A. Belkin and Y. R. Shen, Phys. Rev. Lett. **91**, 213907 (2003).
[16]O. Quinet and B. Champagne, J. Chem. Phys. **115**, 6293 (2001).
[17]O. Quinet and B. Champagne, Int. J. Quantum Chem. **89**, 341 (2002).

[18]D. Rappoport and F. Furche, J. Chem. Phys. **126**, 201104 (2007).
[19]J. Guthmuller, F. Cecchet, D. Lis, Y. Caudano, A. A. Mani, P. A. Thiry, A. Peremans, and B. Champagne, ChemPhysChem **10**, 2132 (2009).
[20]F. Cecchet, D. Lis, Y. Caudano, A. A. Mani, A. Peremans, B. Champagne, and J. Guthmuller, J. Phys.: Condens. Matter **24**, 124110 (2012).
[21]A. A. Mani, Z. D. Schultz, Y. Caudano, B. Champagne, C. Humbert, L. Dreesen, A. A. Gewirth, J. O. White, P. A. Thiry, and A. Peremans, J. Phys. Chem. B **108**, 16135 (2004).
[22]F. Cecchet, D. Lis, J. Guthmuller, B. Champagne, G. Fonder, Z. Mekhalif, Y. Caudano, A. A. Mani, P. A. Thiry, and A. Peremans, J. Phys. Chem. C **114**, 4106 (2010).
[23]I. Benjamin, Phys. Rev. Lett. **73**, 2083 (1994).
[24]A. Morita and J. T. Hynes, Chem. Phys. **258**, 371 (2000).
[25]A. Morita and J. T. Hynes, J. Phys. Chem. B **106**, 673 (2002).
[26]A. Perry, H. Ahlborn, B. Space, and P. B. Moore, J. Chem. Phys. **118**, 8411 (2003).
[27]P. J. Feibelman, Chem. Phys. Lett. **389**, 92 (2004).
[28]A. Morita, Chem. Phys. Lett. **398**, 361 (2004).
[29]M. G. Brown, D. S. Walker, E. A. Raymond, and G. L. Richmond, J. Phys. Chem. B **107**, 237 (2003).
[30]V. Buch, J. Phys. Chem. B **109**, 17771 (2005).
[31]Y. L. Yeh, C. Zhang, H. Held, A. M. Mebel, X. Wei, S. H. Lin, and Y. R. Shen, J. Chem. Phys. **114**, 1837 (2001).
[32]M. A. Belkin, T. A. Kulakov, K. H. Ernst, L. Yan, and Y. R. Shen, Phys. Rev. Lett. **85**, 4474 (2000).
[33]R.-H. Zheng and W.-M. Wei, J. Phys. Chem. B **111**, 1431 (2007).
[34]M. A. Belkin, Ph.D. thesis, University of California, Berkeley, 2004.
[35]X. Zhuang, P. B. Miranda, D. Kim, and Y. R. Shen, Phys. Rev. B **59**, 12632 (1999).
[36]M. J. Frisch, G. W. Trucks, H. B. Schlegel *et al.*, Gaussian 09, Revision A.01, Gaussian, Inc., Wallingford, CT, 2009.
[37]D. A. Pearlman, D. A. Case, J. W. Caldwell, W. S. Ross, T. E. Cheatham, S. Debolt, D. Ferguson, G. Seibel, and P. Kollman, Comput. Phys. Commun. **91**, 1 (1995).
[38]J. M. Wang, R. M. Wolf, J. W. Caldwell, P. A. Kollman, and D. A. Case, J. Comput. Chem. **25**, 1157 (2004).
[39]D. van derSpoel, E. Lindahl, B. Hess, A. R. van Buuren, E. Apol, P. J. Meulenhoff, D. P. Tieleman, A. L. T. M. Sijbers, K. A. Feenstra, R. van Drunen, and H. J. C. Berendsen, Gromacs User Manual, version 4.5, 2010, see www.gromacs.org.
[40]D. J. Adams and G. S. Dubey, J. Comput. Phys. **72**, 156 (1987).
[41]A. J. Moad and G. J. Simpson, J. Phys. Chem. B **108**, 3548 (2004).